RESEARCH ARTICLE

NANO · MICRO small
www.small-journal.com

Neutral MOF Anion Receptor: Radical-Promoted Precise Anion Recognition

Shuyu Dong, Zhiwu Yu, Liecheng Guo, Yuting Yang, Changzheng Tu, Rajamani Krishna, and Feng Luo**

Precise ion recognition plays a key role in the anionic decontamination in water. However, the established anionic recognition based on neutral or cationic anion receptor is still restricted by the inherent limitation, such as narrow application scope in organic solvent rather than water for neutral anion receptor and poor selectivity due to non-directional electrostatic interaction for cationic anion receptor. Herein, for the first time, a neutral metal–organic framework (MOF) anion receptor is shown, enabling precise anion recognition, for example, the presence of a variety of 1000-fold competitive anions does not affect the selective adsorption of the target anion at all. A radical-dominating anion-recognition mechanism is proposed for rationalizing the efficacy of the neutral MOF.

1. Introduction

Anions play a pivotal vital in our daily lives.[1–3] For example, DNA, our genetic origin, is anionic. Iodine is necessary for the synthesis of thyroid hormone. Fluorine is an indispensable component in bones or teeth.[1] On the other side, anions also have adverse influence on the environment and our lives.[3] Commonly, anionic pollutants in water include nitrate, sulfate, phosphate, chromate, arsenate, and pertechnetate.[3] Nitrate and sulfate make the major contribution for the formation of acid rain.[3] A large amount of phosphate can cause red tides and algal blooms, seriously harming marine animals and ecological balance.[3] Chromate and arsenate, typical heavy metal pollutants, could lead to serious health hazards.[3e] Pertechnetate ($^{99}TcO_4^-$), a by-product of nuclear fuel reprocessing, results in dual hazards of metal toxicity and long-life radioactivity.[4] Accordingly, there is still a large and long-term motivation for investigating anion recognition with a purpose of detection, sensing, and capture.[5,6]

Anions are usually larger in size than their isoelectronic cations, and thus exert smaller Coulombic interactions with the host. And, water will be one of the most strong competitor, and could be facile to occupy the advantageous position originally used to bind anion in a host–guest system. In addition, in the actual polluted water, the target anion also faces strong competition from diverse other anions that are invariably present. All these disadvantages make the difficulty for anion recognition. Accordingly, a challenging objective is to design and synthesize matchable receptor for anion recognition. Generally, cationic anion receptors represent a prime scheme, relying on the electrostatic interaction of host–guest chemistry.[7–10] However, such an approach is still majorly blocked by the poor selectivity toward target anion caused by the non-directional nature remains. In principle, neutral counterpart could overcome such a disadvantage.[11–13] However, the success in this strategy mainly existed in polar organic solvents, rather than water, thus seriously restricting its practical application such as anion pollution in water, mainly due to the non-electrostatic driver.

Hydrogen bonding and anion–π interaction in the host–guest system have been found to crease the affinity toward anion.[5,6,14] Following in this direction, several new cationic anion receptors, for example, metal–organic frameworks (MOFs), covalent organic frameworks, and porous organic polymers have been exploited,[15–20] due to its confined space and functionalized pore wall capable of optimizing supramolecular interactions in the host–guest system. However, a crucial issue remains the selectivity toward target anion, which will be significantly reduced in the presence of a large number of competitive anions, mainly due to its inherently non-directional electrostatic nature.

Given the advantage in both cationic and neutral anion receptors, a combination of them could afford an ideal solution for anion recognition. With this concept in our mind, we developed herein a neutral MOF, ECUT-300, that has a weak charged nature resulting from the persistent radical cation. These unique

S. Dong, L. Guo, F. Luo
School of Chemistry
Biology and Materials Science
East China University of Technology
Nanchang 330013, P. R. China
E-mail: luofengaiqi@ecut.edu.cn
Z. Yu
High Magnetic Field Laboratory Chinese Academy of Sciences Hefei
Hefei, Anhui 230031, P. R. China
Y. Yang, C. Tu
College of Chemistry and Environmental Science
Qujing Normal University
Qujing 655011, P. R. China
E-mail: yangyt201411@163.com
R. Krishna
Van't Hoff Institute for Molecular Sciences
University of Amsterdam
Science Park 904, Amsterdam 1098 XH, The Netherlands

The ORCID identification number(s) for the author(s) of this article can be found under https://doi.org/10.1002/smll.202304054

DOI: 10.1002/smll.202304054

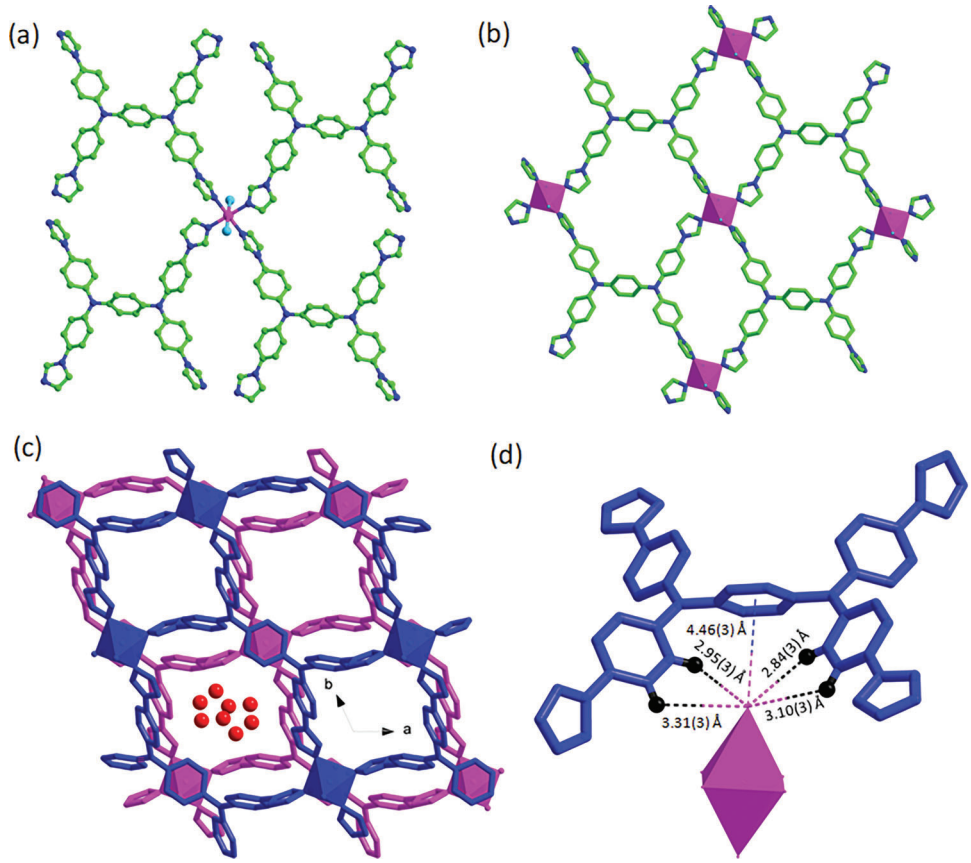

Figure 1. a) The coordination surrounding around metal ions. color code: C/green, N/blue, Co/purple, Cl/cyan. All hydrogen atoms are omitted for clarity. b) View of the sql net constructed by Co(II) ions and L ligands. c) View of the 3D stacking architecture showing 1D channel along *c* direction with occupied free water molecules (red ball). d) View of the interlayer supramolecular interactions composed of C—H…Cl hydrogen bonds and Cl^{-}–π interactions.

features endowed this MOF to exhibit benchmark selectivity toward ReO_4^- over other competitive anions such as Cl^-, NO_3^-, CO_3^{2-}, SO_4^{2-}, $H_2PO_4^{2-}$, and HCO_3^- in the 1000-fold amount, suggesting its superior application in removal of radioactive anion of pertechnetate (TcO_4^-).

2. Results and Discussion

2.1. Synthesis and Structure

ECUT-300 was synthesized by the solvothermal self-assembly of $Co(NO_3)_2$ with a multiple nitrogen-donor ligand of *N*,[1] *N*,[1] *N*,[4] *N*[4]-tetrakis(4-(1H-imidazol-1-yl)phenyl)benzene-1,4-diamine (L) in the presence of little HCl at 120° for 3 days. A detailed description of the synthesis of L and MOF was included in the Supporting Information.

The structure of ECUT-300 was determined by single crystal X-ray diffraction, giving a low symmetry crystal system with P-1 space group, and chemical formula, $Co(L)(\mu\text{-}Cl)_2 \cdot 8H_2O$, where the amount of water molecules was confirmed by TG test (Figure S1, Supporting Information). Within ECUT-300, the positive charge of each Co(II) ion was balanced by two terminal coordinated Cl^- ions, implying an overall neutral net. The unit cell contains one crystallography-independent Co(II) site, which affords an elongated octahedron geometry, finished by four L nitrogen atoms with shorter Co—N bonds (2.049(7)–2.071(7)Å), and two μ-Cl^- ions with longer Co—Cl bonds (2.728(3) Å) (**Figure 1**a). L ligand takes a tetradentate mode to bind with four Co(II) ions. A 2D sql net is built through the combination of Co(II) and L ligands, as shown in Figure 1b, and further interlayer supramolecular interactions create a 3D stacking architecture with 1D channel along *c* direction, which is occupied by free water molecules (Figure 1c,d).

2.2. Characterization of Radical

Noteworthily, the samples of ECUT-300 afforded strong EPR signal at $g = 2.006$, which are assigned to $L^{+\cdot}$ radical cation from the p orbital splitting of N atoms,[21] and the observation of broad signals with hyperfine splitting at low fields was contributed from Co(II) ions. More impressively, such cation radical showed ultrahigh stability in both thermal and water conditions, such as thermostability up to 200 °C and water stability as long as 3 months (**Figure 2**a,b). To the best of knowledge, such high stability of radical observed in ECUT-300 is still scarce.[22–24] Interestingly, we also found that the amount of radical cation can be further boosted by radical when ECUT-300 was exposed to

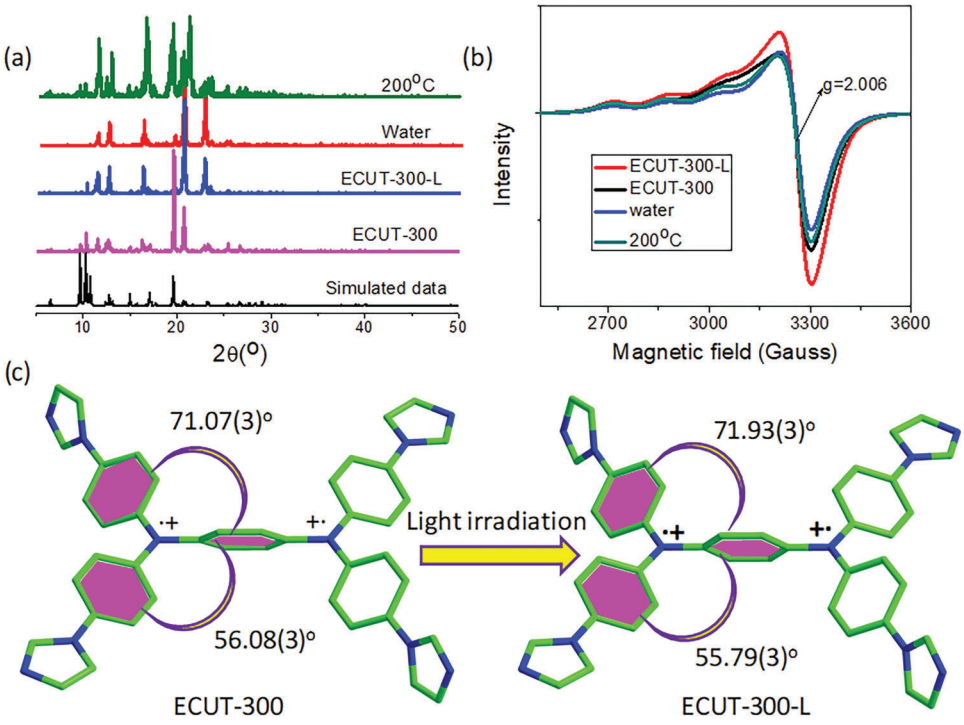

Figure 2. a,b) A comparison of PRXD patterns and ESR signals among the simulated one from single crystal data of ECUT-300, as-synthesized samples of ECUT-300, samples of ECUT-300-L, samples of ECUT-300 after soaking in water for 3 months, and samples of ECUT-300 after heating for 200 °C. c) A comparison in the structure of L ligand before and after light irradiation.

xenon lamp source under ambience (Figure 2a,b). To distinguish with the pristine samples, the samples after light irradiation were named as ECUT-300-L. And, a significant change in dihedral angle of $L^{+\cdot}$ radical cation was observed in ECUT-300-L (71.93(3)°) (Figure 2c), relative to ECUT-300 (71.07(3)°), which could be responsible for the light-promoted radical cation observed in ECUT-300-L.

The surface charge of ECUT-300 was investigated by Zeta potential, giving +63.3 mV at pH = 5 (Figure S2, Supporting Information). Such results reveal a weak positive charge of the skeleton of ECUT-300, which is in line with the fact that ECUT-300 owns a neutral skeleton but with a local and weak positive charge from $L^{+\cdot}$ radical cation. Notably, the weak positive surface charge of ECUT-300 was still maintained after heating 200 °C or soaking in water for 3 months, in good agreement with the results of thermal and water stability tests. Moreover, the samples after light irradiation, ECUT-300-L, gave a Zeta potential of +74.5 mV (Figure S2, Supporting Information), bigger than that in ECUT-300, owing to a light-induced enhancement in the amount of radical cation.

2.3. ReO_4^- Capture

Given that the neutral skeleton with weak local positive charge, and ultrahigh thermal and water stability for such $L^{+\cdot}$ radical cation, as well as light-boosted radical cation, ECUT-300 possibly as an ideal anion receptor with the combination of neutral and cationic anion receptor is suggested. To confirm this, ReO_4^- ion was selected for investigation of anion recognition. Generally, the research ReO_4^- ion recognition was mainly driven by its alternative research for radioactive and toxic $^{99}TcO_4^-$, because of their comparable physical and chemical properties. A major challenge in the recognition and then removal of $^{99}TcO_4^-$ remains that the competing anion will significantly reduce the recognition of $^{99}TcO_4^-$ in the case of the amount of competing anions more than 100-fold.[15–20] For example, the current benchmark material, SCU-CPN-2, afforded a recorded ReO_4^- uptake, but its recognition toward ReO_4^- is largely reduced up to 50%, in the presence of 100-fold competing SO_4^- ion.[25] This is mainly due to the use of cationic framework in the literature, which inherently inherits a non-directional electrostatic interaction of host–guest chemistry and consequently poor selectivity.

We initially investigated the adsorption kinetics for a 50 ppm ReO_4^- solution (**Figure 3**a). A rapid adsorption equilibrium within 2 h was observed for ECUT-300. The removal efficiency is about 70%. The sorption data obeys the pseudo-second–order model with $R^2 > 0.998$, suggesting a chemical adsorption from an electrostatic plus supramolecular interactions between MOF skeleton and ReO_4^- ions.[26] In contrast to the pristine sample of ECUT-300, the samples after light irradiation, ECUT-300-L, gave an increase up to 98% in the removal efficiency under comparable adsorption equilibrium time. Compared to the established solid adsorbents,[15–20] our case represents the first example of boosting ReO_4^- uptake by external stimuli, rather than design and construction of new adsorbents.

Subsequently, we tested the adsorption capacity of ECUT-300 and ECUT-300-L for a ReO_4^- solution with the initial concentration of 10–500 ppm (Figure 3b). ECUT-300 gave 195 mg g^{-1}, while ECUT-300-L performed 315 mg g^{-1}, a 1.6-fold

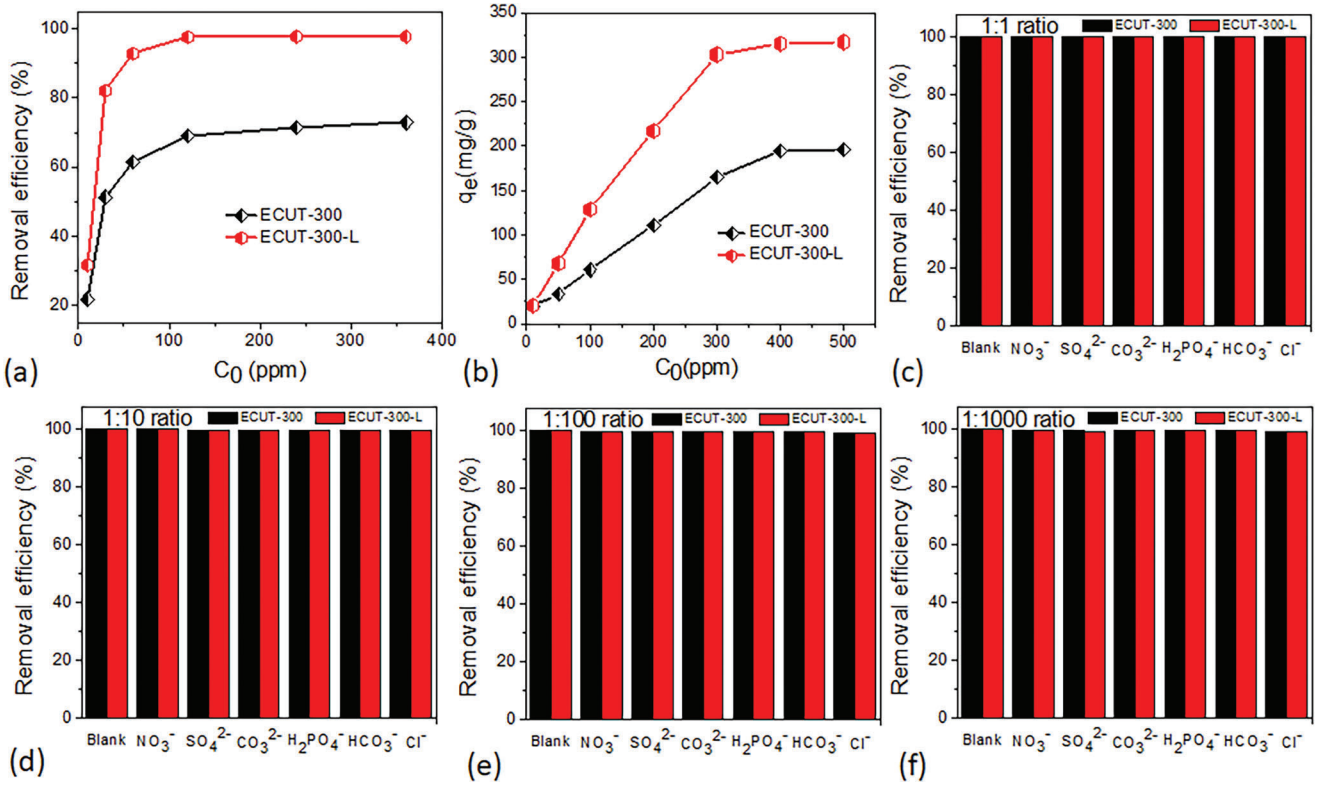

Figure 3. a) Adsorption kinetics of ECUT-300 and ECUT-300-L. b) Adsorption isotherms of ECUT-300 and ECUT-300-L. c–f) Selective adsorption of ReO_4^- with other competing ions in the respectively 1:1, 1:10, 1:100, and 1:1000 ratio.

enhancement in the ReO_4^- uptake under light irradiation. Such uptake values in both ECUT-300 and ECUT-300-L are comparable with that observed in most reported cationic MOFs.[26] However, our investigations represent the first neutral MOF with high ReO_4^- uptake.

The ReO_4^- adsorption selectivity upon ECUT-300 and ECUT-300-L was first explored for a 1:1 binary mixed solution containing 10 ppm ReO_4^- ion and 10 ppm of competing ions such as Cl^-, NO_3^-, SO_4^{2-}, CO_3^{2-}, $H_2PO_4^-$, and HCO_3^- (Figure 3c). In contrast to the blank (1:0) showing more than 99.9% removal efficiency, the presence of 1:1 competing ion showed no impact at all on the removal efficiency. More impressively, enlarging the ratio of competing ions to target ion to 1:10, 1:100, and even 1:1000 still showed no detectable influence in the ReO_4^- removal efficiency (Figure 3d–f). Notably, such remarkable ReO_4^- selectivity surpasses all established adsorbents for ReO_4^- uptake.[15–20] The ReO_4^- affinity in such host–guest system for these mixed solution (1:1, 1:10, 1:100, and 1:1000), estimated from distribution coefficient, K_d value, was at least 1.0×10^6 mg L^{-1} for both ECUT-300 and ECUT-300-L, indicative of strong affinity toward ReO_4^- ion from such neutral MOF with $L^{+\cdot}$ radical cation.

Desorption experiments were conducted using 3 M $NaNO_3$ eluent, resulting in 98% desorption efficiency. Then, an adsorption–desorption cycle was repeated five times (Figure S3, Supporting Information), and no clear decrease in the ReO_4^- uptake was observed, indicating good reusability. Moreover, we further measured the pH effect in the range of pH = 1–12 (Figure S4, Supporting Information). It is found that the ReO_4^- uptake was not affected at pH > 5, while it would significantly affected at pH < 5, suggesting its application scope at weak neutral and alkaline environments.

2.4. Mechanism of ReO_4^- Recognition

To disclose the adsorption mechanism, we first measured the PXRD pattern of cargo loading samples. Clearly, a comparable PXRD pattern was observed between ReO_4^--loaded and pristine samples (Figure S5, Supporting Information), suggesting the retention of MOF structure after ReO_4^- loading. The observation of EPR signal at $g = 2.006$ revealed the retention of $L^{+\cdot}$ radical cation after ReO_4^- loading (Figure S6, Supporting Information). New peak of IR spectra at 937 cm^{-1} belongs to Re—O asymmetric stretch (Figure S7, Supporting Information).[25] More impressively, we can successfully determine the structure of ReO_4^--loaded samples through single crystal X-ray diffraction (**Figure 4**). No obvious change in the MOF skeleton was observed in the ReO_4^--loaded samples, compared with ECUT-300-L. The positive charge of Co(II) was still balanced by two μ-Cl^- ions, while ReO_4^- ions was confined in the 1D channel, showing multiple supramolecular interactions with MOF skeleton (Figure 4), such as C—H...O hydrogen bonds (1.95(3)–3.15(3)Å) and anion–π interactions (3.40(3)–4.01(3)Å). These results reveal that the weak positive charge from $L^{+\cdot}$ radical cation and the exact spatial confinement from both hydrogen bonds and anion–π interactions make the prime contribution to the precise recognition

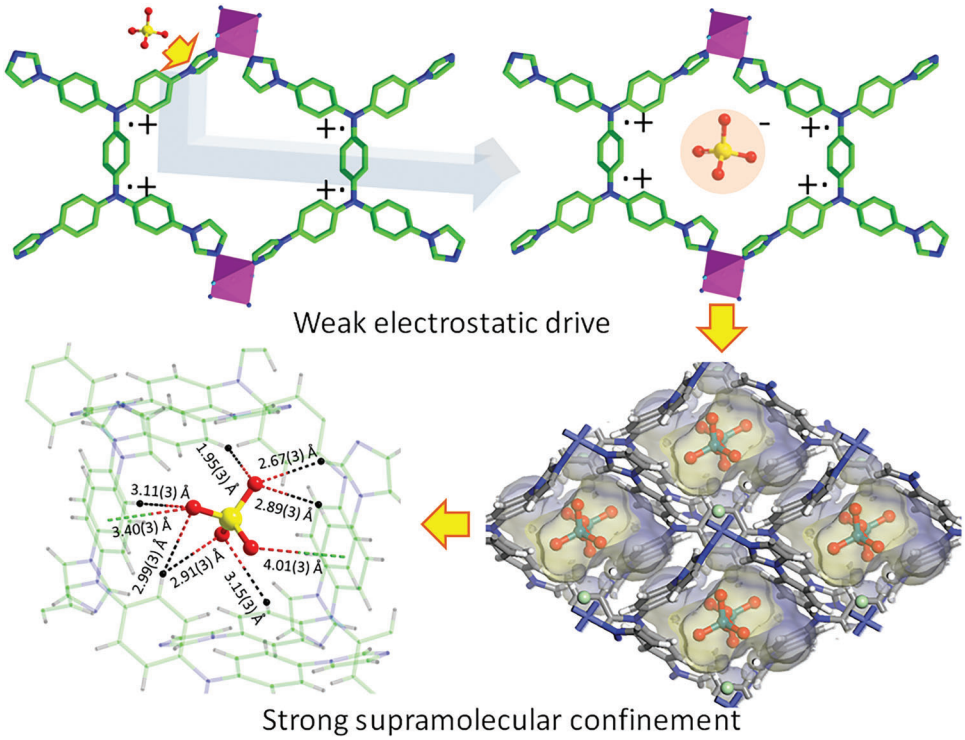

Figure 4. View of the mechanism for current neutral MOF anion receptor showing a precise recognition toward ReO_4^- in water, where a collaboration mechanism from the weak electrostatic drive and strong supramolecular confinement is proposed.

toward ReO_4^- ion by such a neutral MOF anion receptor, ECUT-300 and ECUT-300-L, which finally overcame the disadvantage in both neutral and cationic anion receptors.

3. Conclusion

In summary, we have successfully demonstrated a neutral MOF receptor that can perform a precise recognition toward ReO_4^- ion in water. It's ReO_4^- affinity and consequently adsorption selectivity was remarkable even under the presence of a variety of 1000-fold competing ions, suggesting its huge potential in treating $^{99}TcO_4^-$-containing radioactive wastewater. The developed MOF afforded ultrahigh thermal and water stability in the aspect of both MOF skeleton and $L^{+\cdot}$ radical cation, and also enabled an unprecedented light-promoted radical; all this makes a crucial support for such precise recognition and capture. Furthermore, the unique adsorption mechanism in this work, derived from a collaboration of persistent radical cation and exact spatial constraint, opens up opportunities in the fundamental design of neutral MOF anion receptor with advanced application in anion recognition in water.

Supporting Information

Supporting Information is available from the Wiley Online Library or from the author.

Acknowledgements

This work was supported financially by the Youth leading talent project of FuZhou (NO. 2020ED64), the National Natural Science Foundations of China (21966002), and the Jiangxi project (DHSQT22021007).

Conflict of Interest

The authors declare no conflict of interest.

Author Contributions

S.D., Z.Y., and L.G. contributed equally to this work. F.L., Y.T.Y., and R.K. supervised and conceived this project and wrote the paper. S.Y.D. did the majority of the experiments and wrote the paper. Z.W.Y., L.C.G., and C.Z.T. did part experiment.

Data Availability Statement

The data that support the findings of this study are available in the supplementary material of this article.

Keywords

anion recognition, neutral anion receptors, neutral metal–organic framework anion receptors, persistent radical cation, TcO_4^- removal

Received: May 15, 2023
Revised: July 10, 2023
Published online: July 19, 2023

[1] S. M. Rowe, S. Miller, E. J. Sorscher, *N. Engl. J. Med.* **2005**, *352*, 1992.
[2] F. Delange, *Thyroid* **1994**, *4*, 107.
[3] a) M. Cametti, K. Rissanen, *Chem. Commun.* **2009**, 2809; b) S. G. Chang, D. Littlejohn, K. Y. Hu, *Science* **1987**, *237*, 756; c) B. Moss, *Chem. Ind.* **1996**, 407; d) P. K. Dasgupta, J. V. Dyke, A. B. Kirk, W. A. Jackson, *Environ. Sci. Technol.* **2006**, *40*, 6608; e) M. Luo, Y. Xiong, H. Wu, X. Feng, J. Li, F. Luo, *Angew. Chem., Int. Ed.* **2017**, *56*, 16376.
[4] a) K. Yoshihara, *Top. Curr. Chem.* **1996**, *176*, 17; b) S. Dong, Y. Zhan, Y. Xia, Q. Zhang, L. Gong, L. Zhang, F. Luo, *Small* **2023**, *19*, 2301001; c) Y. Xu, Z. Yu, Q. Zhang, F. Luo, *Adv. Sci.* **2023**, *10*, 2300408.
[5] N. H. Evans, P. D. Beer, *Angew. Chem., Int. Ed.* **2014**, *53*, 11716.
[6] M. J. Langton, C. J. Serpell, P. D. Beer, *Angew. Chem., Int. Ed.* **2016**, *55*, 1974.
[7] Q. He, G. I. Vargas-Zúñiga, S. H. Kim, S. K. Kim, J. L. Sessler, *Chem. Rev.* **2019**, *119*, 9753.
[8] R. Hein, A. Docker, J. J. Davis, P. D. Beer, *J. Am. Chem. Soc.* **2022**, *144*, 8827.
[9] a) C. H. Park, H. E. Simmons, *J. Am. Chem. Soc.* **1968**, *90*, 2431; b) F. P. Schmidtchen, *Angew. Chem., Int. Ed. Engl.* **1977**, *16*, 720; c) E. Graf, J. M. Lehn, *J. Am. Chem. Soc.* **1976**, *98*, 6403.
[10] J. H. Oh, B. P. Hay, V. M. Lynch, H. Li, J. L. Sessler, S. K. Kim, *J. Am. Chem. Soc.* **2022**, *144*, 16996.
[11] M. A. Yawer, V. Havel, V. Sindelar, *Angew. Chem., Int. Ed.* **2015**, *54*, 276.
[12] K. Hamashima, J. Yuasa, *Angew. Chem., Int. Ed.* **2022**, *61*, e202113914.
[13] S. J. Pike, J. J. Hutchinson, C. A. Hunter, *J. Am. Chem. Soc.* **2017**, *139*, 6700.
[14] M. J. Hao, Z. S. Chen, H. Yang, G. I. N. Waterhouse, S. Q. Ma, X. K. Wang, *Sci. Bull.* **2022**, *67*, 924.
[15] D. Ogata, J. Yuasa, *Angew. Chem., Int. Ed.* **2019**, *58*, 18424.
[16] J. Li, X. Dai, L. Zhu, C. Xu, D. Zhang, M. A. Silver, P. Li, L. H. Chen, Y. Z. Li, D. W. Zuo, H. Zhang, C. L. Xiao, J. Chen, J. Diwu, O. K. Farha, T. E. Albrecht-Schmitt, Z. F. Chai, S. A. Wang, *Nat. Commun.* **2018**, *9*, 3007.
[17] P. Bai, Z. Y. Dong, S. A. Wang, X. Y. Wang, Y. Li, Y. Z. Wang, Y. H. Ma, W. F. Yan, X. D. Zou, J. H. Yu, *Angew. Chem., Int. Ed.* **2020**, *59*, 19539.
[18] Q. Sun, L. Zhu, B. Aguila, P. K. Thallapally, C. Xu, J. Chen, S. Wang, D. Rogers, S. Ma, *Nat. Commun.* **2019**, *10*, 1646.
[19] J. Li, B. Y. Li, N. N. Shen, L. X. Chen, Q. Guo, L. Chen, L. W. He, X. Dai, Z. F. Chai, S. A. Wang, *ACS Cent. Sci.* **2021**, *7*, 1441.
[20] N. N. Shen, Z. Yang, S. Liu, X. Dai, C. Xiao, K. Taylor-Pashow, D. E. Li, C. Yang, J. Li, Y. G. Zhang, M. X. Zhang, R. H. Zhou, Z. F. Chai, S. A. Wang, *Nat. Commun.* **2020**, *11*, 5571.
[21] Y. Cheng, W. Jia, X. Wu, X. Ding, X. Liu, B. Han, *Appl. Catal., B* **2022**, *306*, 121110.
[22] X. Ye, L. Chung, K. Li, S. Zheng1, Y. Wong, Z. Feng, Y. He, D. Chu, Z. Xu, L. Yu, J. He, *Nat. Commun.* **2022**, *13*, 6116.
[23] S. Zhang, L. Ma, W. Ma, L. Chen, K. Gao, S. Yu, M. Zhang, L. Zhang, G. He, *Angew. Chem., Int. Ed.* **2022**, *61*, e202209054.
[24] L. Ji, J. Shi, J. Wei, T. Yu, W. Huang, *Adv. Mater.* **2020**, *32*, 1908015.
[25] J. Li, L. Chen, N. Shen, R. Xie, M. V. Sheridan, X. Chen, D. Sheng, D. Zhang, Z. Chai, S. Wang, *Sci. China: Chem.* **2021**, *64*, 1251.
[26] a) H. Feng, X. H. Xiong, L. L. Gong, H. P. Zhang, Y. Xu, X. F. Feng, F. Luo, *Nano Res.* **2022**, *15*, 1472; b) D. P. Sheng, L. Zhu, X. Dai, C. Xu, P. Li, C. I. Pearce, C. L. Xiao, J. Chen, R. H. Zhou, T. Duan, O. K. Farha, Z. F. Chai, S. A. Wang, *Angew. Chem., Int. Ed.* **2019**, *131*, 5022; c) S. Gu, Z. Yu, N. Li, Q. Zhang, H. Zhang, L. Zhang, L. Gong, R. Krishna, F. Luo, *Chem. Eng. J.* **2023**, *466*, 143139.

NANO · MICRO small

Supporting Information

for *Small*, DOI 10.1002/smll.202304054

Neutral MOF Anion Receptor: Radical-Promoted Precise Anion Recognition

Shuyu Dong, Zhiwu Yu, Liecheng Guo, Yuting Yang, Changzheng Tu, Rajamani Krishna and Feng Luo**

WILEY-VCH

Supporting Information

Neutral MOF Anion Receptor: Radical-Promoted Precise Anion Recognition

Shuyu Dong,[†a] Zhiwu Yu,[†b] Liecheng Guo,[†a] Yuting Yang,[c]* Changzheng Tu,[c] Rajamani Krishna,[d] and Feng Luo[a]*

Corresponding author: Feng Luo, ecitluofeng@163.com, Yuting Yang, yangyt201411@163.com

1. Materials and general methods

All the reagents were purchased from Adamas Reagent, Ltd. and used as received without further purification. X-ray powder diffraction were collected by a Bruker AXSD8 Discover powder diffractometer at 40 kV, 40 mA for Cu Kλ (λ= 1.5406 Å). The simulated powder patterns were calculated by Mercury 1.4. Infrared Spectra (IR) were measured by a Bruker VERTEX70 spectrometer in the 600-4000 cm^{-1} region. The analyses of concentrations of ReO_4^- in the solution was carried out by ThermoFisher iCap7600 ICP-OES instruments. X-ray photoelectron spectra (XPS) were collected by Thermo Scientific ESCALAB 250 Xi spectrometer.

2. Synthesis of L

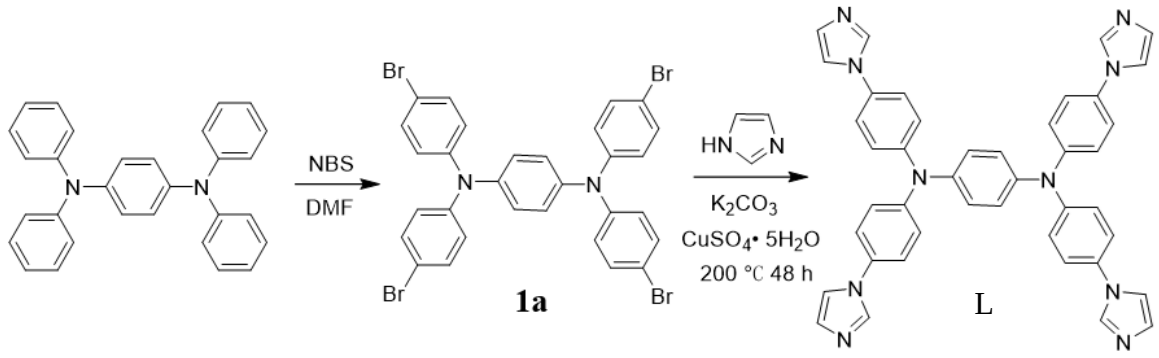

Synthesis of N^1,N^1,N^4,N^4-Tetrakis(4-bromophenyl)benzene-1,4-diamine (**1a**): A solution of N^1,N^1,N^4,N^4-Tetraphenylbenzene-1,4-diamine (0.7g, 1.70 mmol) in dimethylformamide (DMF; 5 mL) was cooled to 0°C. A solution of N-bromo succinimide (NBS, 1.33 g, 7.47 mmol) in DMF (5 mL) was added dropwise, and the temperature was maintained below 5 °C. After addition, the reaction mixture was stirred for 12 h under room temperature. The reaction mixture was then poured into water (500 mL) and filtered, and the residue was washed with methanol for three times. Then, the precipitate was filtered off and dried in vacuum oven at 50 °C to afford the pure product **1a** as a white powder (1.12 g, 93% yield). ^{1}H NMR(400 MHz, $CDCl_3$) δ [ppm]: 7.49 (d, *J* = 8.8 Hz, 8H), 7.19 (d, *J* = 8.8 Hz, 8H), 7,14 (s, 4H).

Synthesis of N^1,N^1,N^4,N^4-tetrakis(4-(1H-imidazol-1-yl)phenyl)benzene-1,4-diamine (L): A sample of **1a** (1.1 g, 1.52 mmol), imidazole (2.2 g, 32.3 mmol), K_2CO_3 (2.2 g, 15.9 mmol), $CuSO_4·5H_2O$ (0.256 g, 1.04 mmol) were mixed and heated at 200 °C for 48 h. Then the reaction mixture was cooled to ambient temperature, and washed several times with water. The remaining solid residue was brought to dryness to give pale green solid L (0.98 g, 1.45 mmol, 95%). ^{1}H NMR(400 MHz, DMSO-d_6) δ [ppm]: 8.35 (d, *J* = 8.8 Hz, 4H), 7.98 (d, *J* = 8.8 Hz, 4H), 7.65 (s, 4H) , 7.31 (s, 8H), 7.20 (s, 8H), 7.17 (s, 4H).

3. Synthesis of ECUT-300

A mixture of L (10 mg) and Co $(NO_3)_2$ (15 mg) in 3 mL DMF and 1 mL acetonitrile in the presence of 250 μL HCl (concentrated hydrochloric acid) was sealed in a Teflon lined Parr autoclave. The solution was heated at 120 °C for 3 days followed by decreasing to room temperature within 2 days. After filtration, block crystals of ECUT-300 were collected as a pure phase. The yield is 67% based on L. Element analysis: Exp. C/53.07%, H/5.06%, N/14.85%, Calc. C/53.06%, H/5.09%, N/14.73%.

4. Synthesis of ECUT-300-L

ECUT-300-L was obtained through exposing the samples of ECUT-300 under xenon lamp under ambience for 1 h. Element analysis: Exp. C/53.04%, H/5.05%, N/14.67%, Calc. C/53.06%, H/5.09%, N/14.73%.

5. X-ray Crystallography

X-ray diffraction data were collected on a Bruker diffractometer at 300 K using graphite monochromated Mo Kα radiation (λ= 0.71073 Å). The data reduction included a correction for Lorentz and polarization effects, with an applied multiscan absorption correction (SADABS). The crystal structure was solved and refined using the SHELXTL program suite. Direct methods yielded all non-hydrogen atoms, which were refined with anisotropic thermal parameters. All hydrogen atom positions were calculated geometrically and were riding on their respective atoms. The SQUEEZE subroutine of the PLATON software suite was used to remove the scattering from the highly disordered guest molecules. CCDC 2260550-2260552 contains the supplementary crystallographic data of these materials, respectively. These data can be obtained free of charge from the Cambridge Crystallographic Data Centre via www.ccdc.cam.ac.uk/ data_request/cif.

6. ReO_4^- uptake experiments

ReO_4^- mother solution was prepared by dissolving 1.44 g NH_4ReO_4 in 1000 mL deionized water to create an 1000 mg/L (ppm) NH_4ReO_4 solution. All the adsorption experiments were conducted at 298 K.

7. ReO_4^- adsorption kinetics

In kinetics experiments, the ReO_4^- solution with initial concentration of 50 ppm was used. The dose of adsorbent is 10 mg, while the used volume of solution is 20 mL.

8. ReO_4^- adsorption isotherms

In isotherm experiments, the ReO_4^- solution with initial concentration of 100-500 ppm was used. The dose of adsorbent is 10 mg, while the used volume of solution is 20 mL and the contact time is 2 h.

The adsorption amount, Q_e (mg/g), was calculated by the difference of the ReO_4^- equilibrium concentration before and after adsorption (see equation 1):

$$Q_e = \frac{(C_0 - C_e) \times V}{m} \qquad (1)$$

where c_0 (mg/L) and c_e (mg/L) are the initial concentration and equilibrium concentration of ReO_4^- in the solutions, respectively; V (mL) is the volume of testing solution and m (mg) is the amount of sorbent.

9. Selectivity

In selective adsorption experiments, a binary mixed solution contains both ReO_4^- and other ion ($NaNO_3$, Na_2CO_3, $NaHCO_3$, NaH_2PO_4, NaCl, Na_2SO_4) with respectively 1:1, 1:10, 1:100, and 1:1000 ratio. The dose of adsorbent is 10 mg, while the solution is 20 mL.

K_d value and selectivity (S) is calculated from the following two equations,

$$K_d = \frac{V}{m} \frac{(C_0 - C_e)}{C_e} \times 10^3 \qquad (2)$$

$$S = \frac{K_d^U}{K_d^M} \qquad (3)$$

where the unit for K_d value is mL/g.

10. Additional Figures and Tables

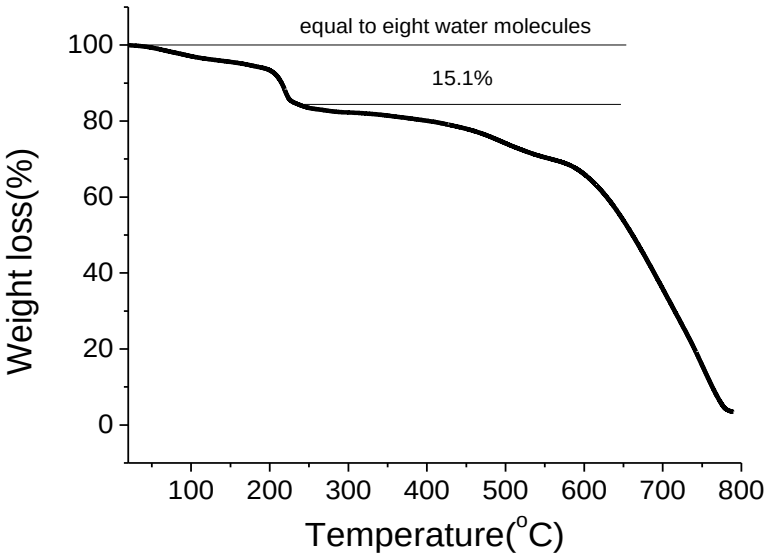

Figure S1. The TG plot of ECUT-300.

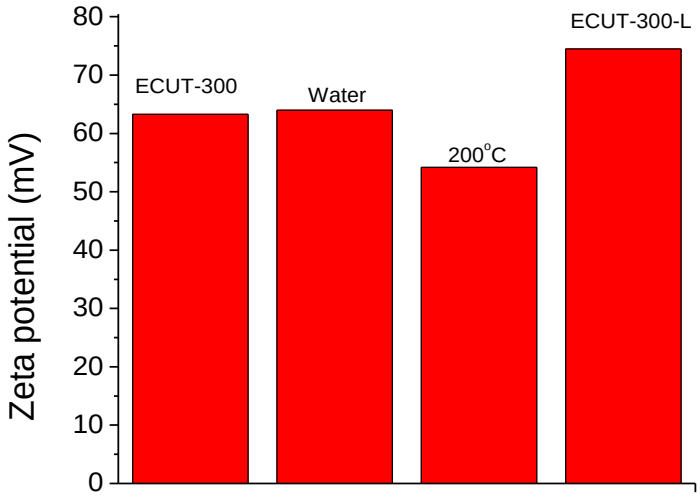

Figure S2. The Zeta potential of these samples at pH=5.

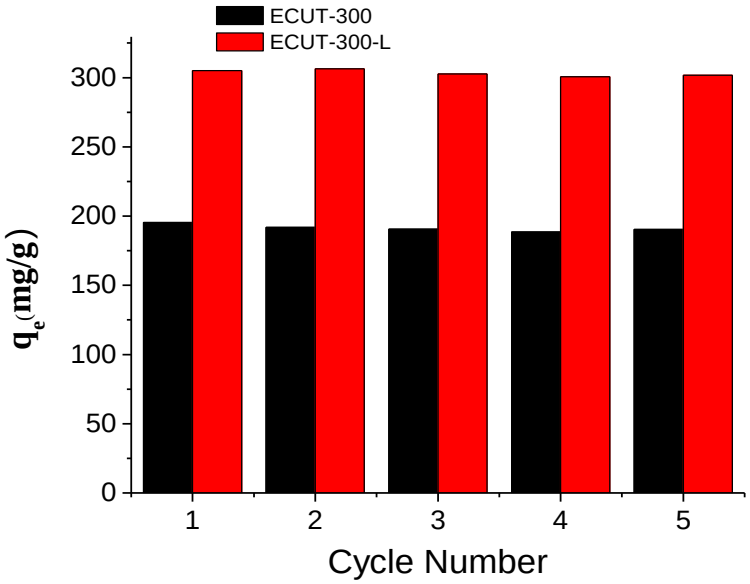

Figure S3. The adsorption-desorption cycle.

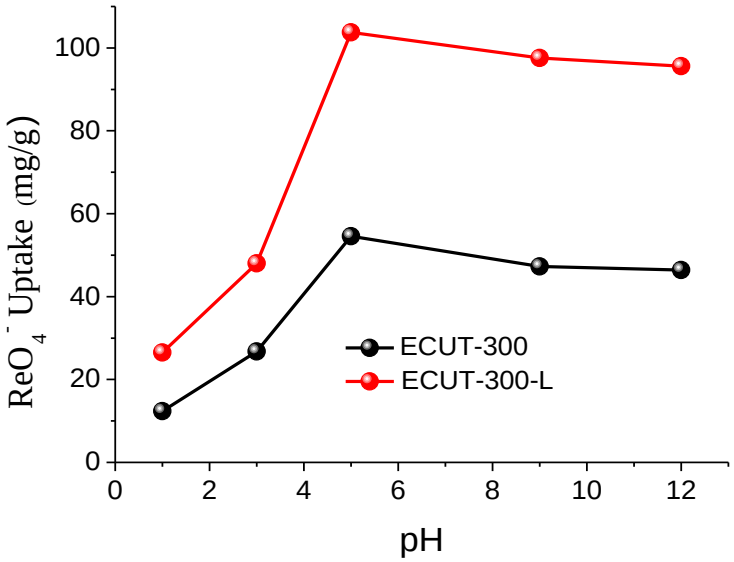

Figure S4. The pH effect on ReO_4^- uptake.

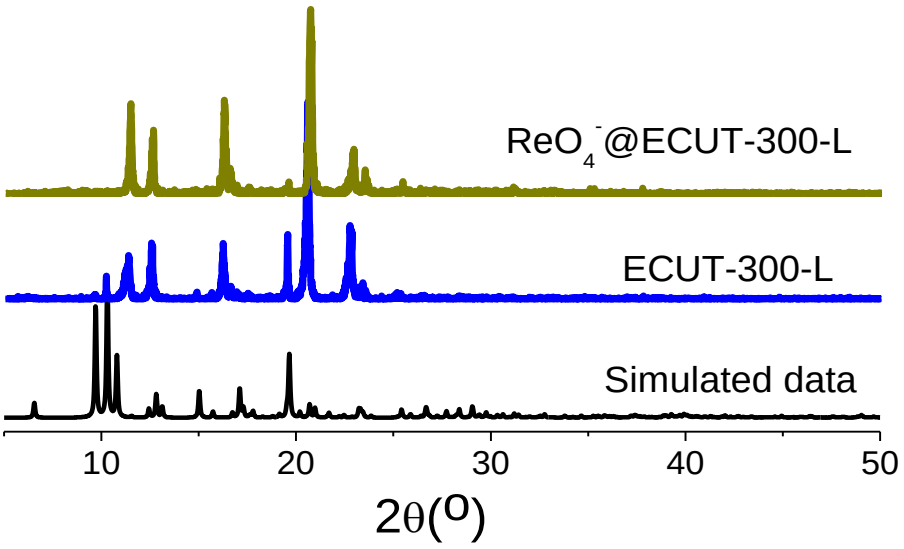

Figure S5. A comparison of PXRD patterns between ECUT-300-L and ReO_4^- loading samples.

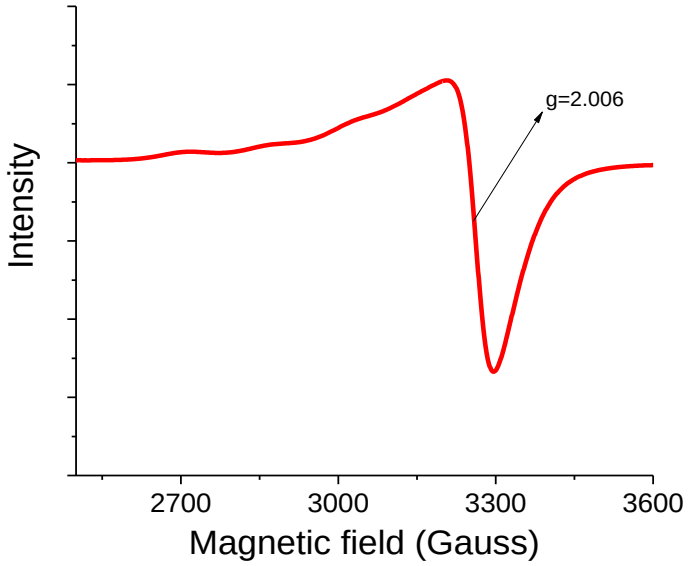

Figure S6. EPR of ECUT-300-L samples after loading ReO_4^-.

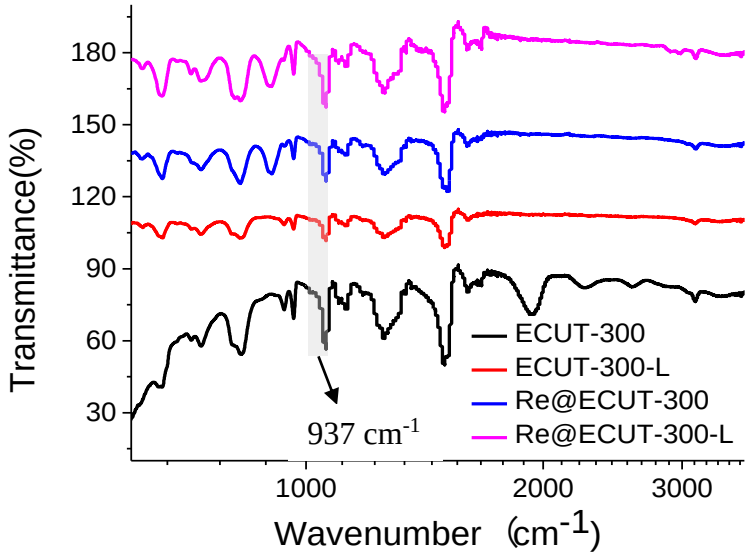

Figure S7. A comparison of IR among ECUT-300, ECUT-300-L, and corresponding ReO_4^- loaded samples.